Digest Journal of Nanomaterials and Biostructures Vol. 9, No. 4, October - December 2014, p. 1399 - 1406

SINGLE MOLECULE LEVEL INVESTIGATIONS ON BONE MORPHOGENETIC PROTEINS BINDING TO GRAPHENE

A. ISTRATE[a], I. APRODU[a], I. BANU[a], , E. VASILE[b], L. PILAN[b], M. IONITA[b*]
[a]*Dunarea de Jos University of Galati, Galati, 8002001, Romania*
[b]*Advanced Polymer Materials Group, University Politehnica of Bucharest, Bucharest, 060042, Romania*

Bone morphogenetic proteins (BMP) have osteoinductive activity and therefore play important roles in overcoming bone disorders. The use of the graphene-based scaffolds in bone tissue engineering appears as a good alternative for the autologous and allogeneic bone grafts, metal alloys or ceramics, which are widely used in case of bone injuries. The aim of the present study was to provide a detailed structural characterization of three different most efficient osteoinductive BMP molecules, and to assess their individual interaction properties with the graphene sheet. The critical amino acids involved in BMP-graphene interactions were identified after performing docking simulations. Although the BMP-2, BMP-6 and BMP-7 share structural similarities, important variation in their affinity for graphene sheet was observed. The interaction force of protein-graphene complexes was estimated by performing unbinding simulations. The highest interaction force (1.31 nN) was obtained in case of the BMP-6 - graphene complex, whereas the BMP-2 - graphene complex has the lowest interaction force (0.25 nN). The information provided here might allow the progress in graphene-based tissue engineering of bones, as well as a better understanding of BMP physiological roles.

(Recieved August 20, 2014; Accepted October 22, 2014)

Keywords: Bone morphogenetic proteins, Graphene, Molecular dynamics, Molecular docking, Interaction properties

1. Introduction

The success of bone tissue engineering highly depends on the functionality of the scaffold. Identifying new scaffold materials with properties like good biocompatibility, controlled non toxic biodegradation, ability to support cell differentiation, growth, and proliferation, and suitable mechanical strength, is crucial for the efficiency of tissue regeneration process [1]. One potential functional scaffold material for bone repair applications is graphene.

Due to the exceptional properties, graphene has many applications. As reviewed by Zhang et al. [2], graphene can be used as scaffold in tissue engineering, for construction of electronic devices, energy storage or conversion systems, etc. Several attempts have been made to functionalize the surface of pristine graphene such as to provide anchoring sites for other molecules [3]. The most common modification of graphene surface concerns the introduction of oxygen containing groups, such as epoxide, hydroxyl and carboxylic groups [2]. The graphene oxide has good solubility, can be easily processed through wet chemical procedures and provides sites for the interaction with different biological molecules. Moreover, graphene properties can be harnessed by incorporating the sheets into composite materials [4]. This approach represents the key for obtaining the new graphene-based material with desired properties for a variety of applications.

In case of bone repair applications the interaction between graphene and peptides or proteins, such as growth factors, is of particular interest. Zhang et al. [2] provided a nice review on the interaction between graphene or graphene oxide and different types of peptides and proteins.

* Corresponding author: mariana_ionita2003@yahoo.com

They highlighted the importance of covalent and non-covalent interactions for proteins immobilization on the flat surfaces. The protein – graphene/graphene oxide conjugates have unique chemical or biological properties, being therefore promising for obtaining novel graphene-based nanoarhitectures [2].

When using graphene-based scaffolds in bone tissue engineering, the interaction with bone morphogenetic proteins (BMP) is crucial. BMP is a subfamily of the transforming growth factor beta superfamily ligands, and includes members able to induce bone formation through controlling different developmental and intercellular signalling processes [5-8]. The osteoinductive properties of BMPs have been studied through molecular biology techniques by recombinant expression of each member.

The present study was focused on three different BMP structures, previously solved through crystallography technique. A comparative structural and conformational analysis on BMP-2, BMP-6 and BMP-7 was performed after running molecular dynamics simulations. In addition, BMP - graphene complexes were generated using protein dedicated docking tools, to identify key amino acid residues involved in protein affinity for the graphene sheet.

2. Materials and methods

2.1 Molecular model

The X-ray crystallographic models of the proteins investigated in the present study have been taken from the Brookhaven Protein Data Bank. Three different bone morphogenetic proteins were considered: 3BMP.pdb model of the BMP-2 at 2.70 Å resolution [5], the 2QCW.pdb model of the BMP-6 at 2.49 Å resolution [8], and the 1LXI.pdb model of the BMP-7 at 2.00 Å resolution [7]. With regard to BMP-6, only one monomer was considered for the simulations.

Before running molecular dynamics and docking simulations all protein models were refined by removing the non-protein chemical compounds, such as (4S)-2-methyl-2,4-pentanediol, which are not present under physiological conditions, and all water molecules.

2.2 Computational set-up

The geometry optimization and molecular dynamics (MD) simulations were carried out using Gromacs 4.5.5 software [9] and GROMOS96 43a1 force field on a Intel(R) Core(TM)2 CPU 6300 1.86 GHz processor-based machine running Linux in parallelization conditions.

The energy of the models was minimized first in vacuum by steepest descent algorithm, and the minimized structures were then centred in rectangular boxes of appropriate size with periodic boundary conditions, to allow mimicking their behaviour. After solvation by adding single point charge (SPC) explicit water molecules, for accurate modelling of the hydrogen bonding, ion-dipole, and dipole-dipole interactions between solvent and protein models, the systems were subjected to a new step of geometry optimization using the same algorithm. Further MD steps were carried out at an integration time step of 2 fs for heating the solvated biological systems, by coupling each component to a Berendsen thermostat, and equilibration at 37^{o}C. The following set-up parameters were used for all MD simulations: neighbour list at 1.7 nm for computing the nonbonding interactions, electrostatic interactions described by the Particle-Mesh-Ewald (PME) method, and van der Waals interactions by the switching function between 0.9 and 1.1 nm.

The outcomes of the MD equilibration steps at 37^{o}C were used for further checking structural particularities and for running docking simulations. The PDBsum [10], LigPlot+ v1.4.5. [11] and VMD packages [12] were employed for detailed analysis of the BMP models.

2.3. Docking procedure

In order to investigate the affinity of the different BMP molecules for graphene sheet, the equilibrated models were used as input for the rigid body docking procedure using the PatchDock

algorithm [13]. The graphene sheet used as receptor in the docking procedure had a diameter of 86 Å. The output of the docking procedure consisted of BMPs - graphene complexes scored based on the geometric fit and atomic contact energy. Further refinement of the rigid-body docking solutions was performed using the FireDock web server, by rearranging the interface side chains and adjustment of the relative orientation of the molecules within complex [14]. The best fits, decided based on the binding energy values which considers both softened attractive and repulsive van der Waals energy, were further equilibrated and used for atomic detail check.

2.4. Determination of the BMP - graphene interaction properties

In order to assess the interaction forces between BMP molecules and graphene sheet, the complexes generated through the docking procedures were optimized at different intermolecular distances (Figure 1), using the same set-up as for the initial protein optimization. The intermolecular distance was estimated as the shortest distance between the interfacial amino acids of BMP molecules and the graphene sheet.

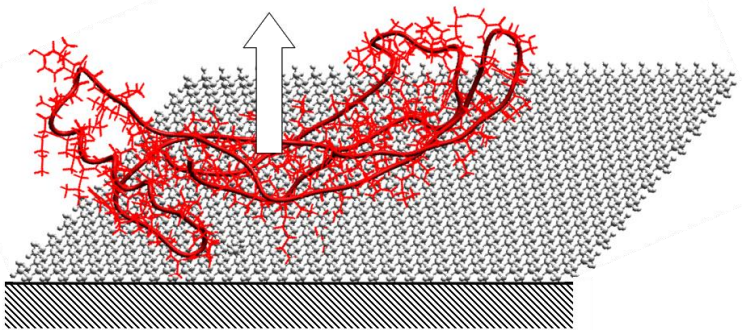

Fig. 1. Scheme of the set-up used for testing the interaction between graphene sheet (represented in grey) and BMP molecules (represented in red). The graphene molecule was kept fixed while the protein was rigidly displaced such as to create different intermolecular distances. The arrow on top of protein indicates the direction of the rigid displacement.

3. Results and discussion

3.1. BMPs characterization at single molecule level

The proteins of the BMP subfamily are responsible for osteoinductive activity, and can be divided in subclasses, as follows: BMP-2 and BMP-4 share a high amount of amino acids and form the first subclass, BMP-5, BMP-6, BMP-7 (known as osteogenic protein 1) and BMP-8 (known as osteogenic protein 2) form the second subclass, whereas the BMP-3 form the third subclass [6, 15].

Among members of BMP subfamily, we focused our attention on BMP-2, BMP-6 and BMP-7, which appear to be the most active players in bone induction [6]. On the other hand BMP-3 was considered to have a negative modulation effect on bone formation [16]. Even if bone matrix contains all types of BMP molecules, it was shown that individual protein might support alone the bone inductive activity [6].

In order to better understand the atomic particularities and interaction with potential scaffold material of some representative BMP molecules, the BMP-2, BMP-6 and BMP-7 models were solvated and equilibrated at temperature resembling the human body conditions.

The analyzed proteins had similar shape and volume (Table 1), and in all cases a cubic box was considered for solvating the protein models. The final size on the complexes highly depended on the total number of water molecules used for proteins solvation (Tabel 1). The size of the box,

which decisively influence the number of water molecules, was decided such as to save computational resources and not to constrain proteins behaviour. Hydrogen bonds within the proteins and between proteins and water molecules were computed with Gromacs software based on cutoffs for the angle hydrogen - donor - acceptor and the distance between donor and acceptor. Analysing the results presented in Table 1, one can see that there is a direct correlation between the total number of water molecules in the system and the hydrogen bonds established with the solute.

Table 1. Overall structure and energy details of BMP-2, BMP-6 and BMP-7 molecules

Parameter	BMP-2	BMP-6	BMP-7
Solvated structure descriptors			
No of atoms	49033	47383	49940
No of water molecules	16107	15576	16432
Overall structure descriptors*			
Volume, nm^3	19.04±0.64	18.70±0.67	18.61±0.69
Hydrophobic, nm^2	43.12±0.80	40.12±0.73	40.04±0.85
Total surface, nm^2	73.08±1.24	67.25±0.98	68.51±1.09
Hb within protein	53±3	62±3	57±3
Hb protein - water	220±7	200±8	314±9
Energy descriptor*			
Potential energy, kJ/mol	-692695.43 ±765.90	-644319.55 ± 632.05	-679815.82 ±674.47
Total energy, kJ/mol	-503015.34 ±677.21	-520921.31 ± 485.16	-549731.18 ±499.35

*Mean values are given with standard deviation
Hb – hydrogen bonds

The reliability and quality of the equilibrated models has been judged based on their stability and stereochemical particularities. The atomic fluctuations of Cα estimated as the root mean square deviation (RMSD) in the last 500 ps of the equilibration step were 0.34±0.02 nm for BMP-2, 0.22±0.02 nm for BMP-6 and 0.40±0.03 nm for BMP-7. Moreover the values of potential and total energy were rather stable (Table 1). On the other hand, the Ramachandran plot statistics indicated high amounts of amino acids with permitted backbone conformations for psi/phi angle pairs for each of the investigated protein. The good reliability of the obtained results is guaranteed by the percentages of residues falling in the most favoured and allowed regions of the diagram [17]: 94.6%, 95.7% and 94.6% for BMP-2, BMP-6 and BMP-7, respectively.

Although BMP molecules exhibit similar osteoinductive activity, the bioinformatics analysis based on FASTA (version 3.4.) sequence alignment showed that BMP-2 shares only 60.2% and 59% amino acids identities with BMP-6 and BMP-7, respectively. Anyway, BMP-2 and BMP-7 molecules appear to have some common cellular receptors termed type I and type II, and may even form crossed heterodimers [5-7]. On the other hand, BMP-6 and BMP-7, which belong to the same subclass, share 87.4% sequence homology with a Smith – Waterman score of 670 [18], and are slightly larger than BMP-2 molecule.

The differences in terms of primary structure of the three investigated proteins highly influence the amino acids involvement in different types of secondary structure motifs. The major motifs in BMPs structure were identified and analyzed through ProMotif program [10]. In all cases the secondary structure is dominated by the strand motif. The BMP-7 and BMP-6 have the highest amount of amino acids (42.3% and 40.4%, respectively) participating to this kind of structural units. Regardless of BMP molecule, the strands are organized into three different antiparallel β sheets, each consisting on two hydrogen bonded strands connected by loops.

No important differences in the helical content of the investigated BMPs, and no helix-helix interaction have been found after performing molecular dynamics equilibrations steps. The unordered secondary structure of all BMP molecules was dominated by the beta turns motifs, followed by beta bulge and gamma turns.

The investigated BMP molecules are members of the highly conserved cystine-knot growth factors super-family [5, 7, 8]. Each BMP molecule has three disulfide bridges (Table 2) that can be classified based on their internal chi angles as right handed (RHS) or left handed (LHS) spirals [19]. Among the disulphide forming cysteine residues of each BMP molecule, at least one belong to a strand (Cys^{111} in BMP-2, Cys^{129} in BMP-6 and Cys^{67} in BMP-7) and a hairpin motif (Cys^{43} in BMP-2, Cys^{60} in BMP-6 and Cys^{104}, Cys^{136} and Cys^{138} in BMP-7). The disulfide bridges are involved in the stabilization of the 3D structure of the monomers, such as to compensate for the lack of hydrophobic core which is specific to the globular proteins [5]. The hydrophobic amino acids are not buried within the protein core but are mainly located at the surface prevailing over the hydrophilic ones. The hydrophobic surface of the BMPs is therefore rather extensive, representing between 58.44 and 59.66% of the total protein surface (Table 1). On the other hand, the dimerization process, when two monomers become connected by an intersubunit disulfide bond, ensures further molecular stabilization of the structures as well as achieving a hydrophobic core [5, 8]. Both helical and β-sheet motifs are involved in the interactions between monomers.

3.2. Analysis of the BMPs - graphene complexes

The most likely three-dimensional structure of the BMP - graphene complexes were generated using a computational docking procedure. The ranking of the docking solutions provided by the PatchDock is made based on shape complementarity, interface shape and sizes of the molecules [20]. Tacking into account that the graphene model used in this study is plane single layered any variability due to the receptor structure or shape is avoided.

For the sake of simplicity only the monomers of the BMP molecules were used as ligands in the docking procedure. Anyway, the intersubunits interactions have been carefully checked for all investigated BMPs, and there is no overlapping with the amino acids in direct contact with the graphene, meaning that no interference and no significant difference should appear when considering the BMP dimmers.

A detailed check of the BMP - graphene complexes was performed before running simulations to investigate the interaction forces characterizing each system. No important differences in terms of the interaction surface were found among the studied BMP molecules. As indicated by the LigPlot+ representations of the analyzed complexes, the amino acids directly facing the two dimensional structure of graphene are 13, 18, 57, 145, 227, and 225 (Figure 2).

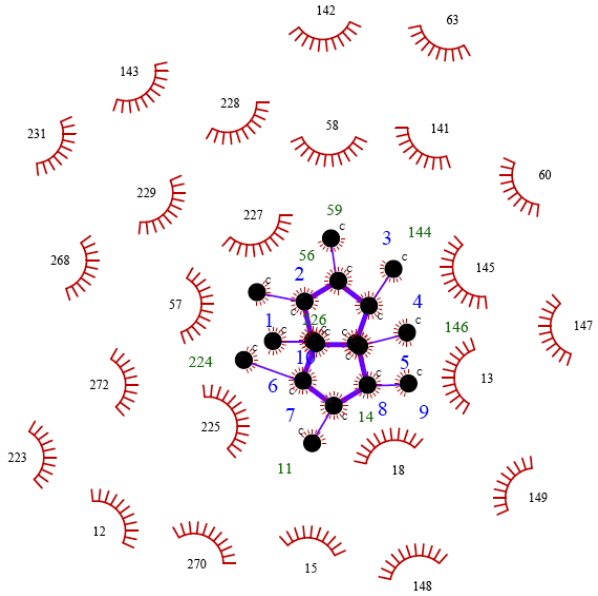

Fig. 2. Contact mapping for the top-scoring BMP-2 - graphene docking solution. The amino acids from the BMP-2 binding surface which are involved in hydrophobic contacts with graphene are represented by an arc with spokes radiating towards the carbon atoms of the graphene layer they contact with. The figure was drawn using LigPlot+.

The affinity of the biomolecules within the BMP - graphene complexes was checked by simulating the unbinding of the complexes. The interaction energy was estimated by subtracting the energy of each component of the complex from the total energy, and was monitored as function of intermolecular distance (Figure 3).

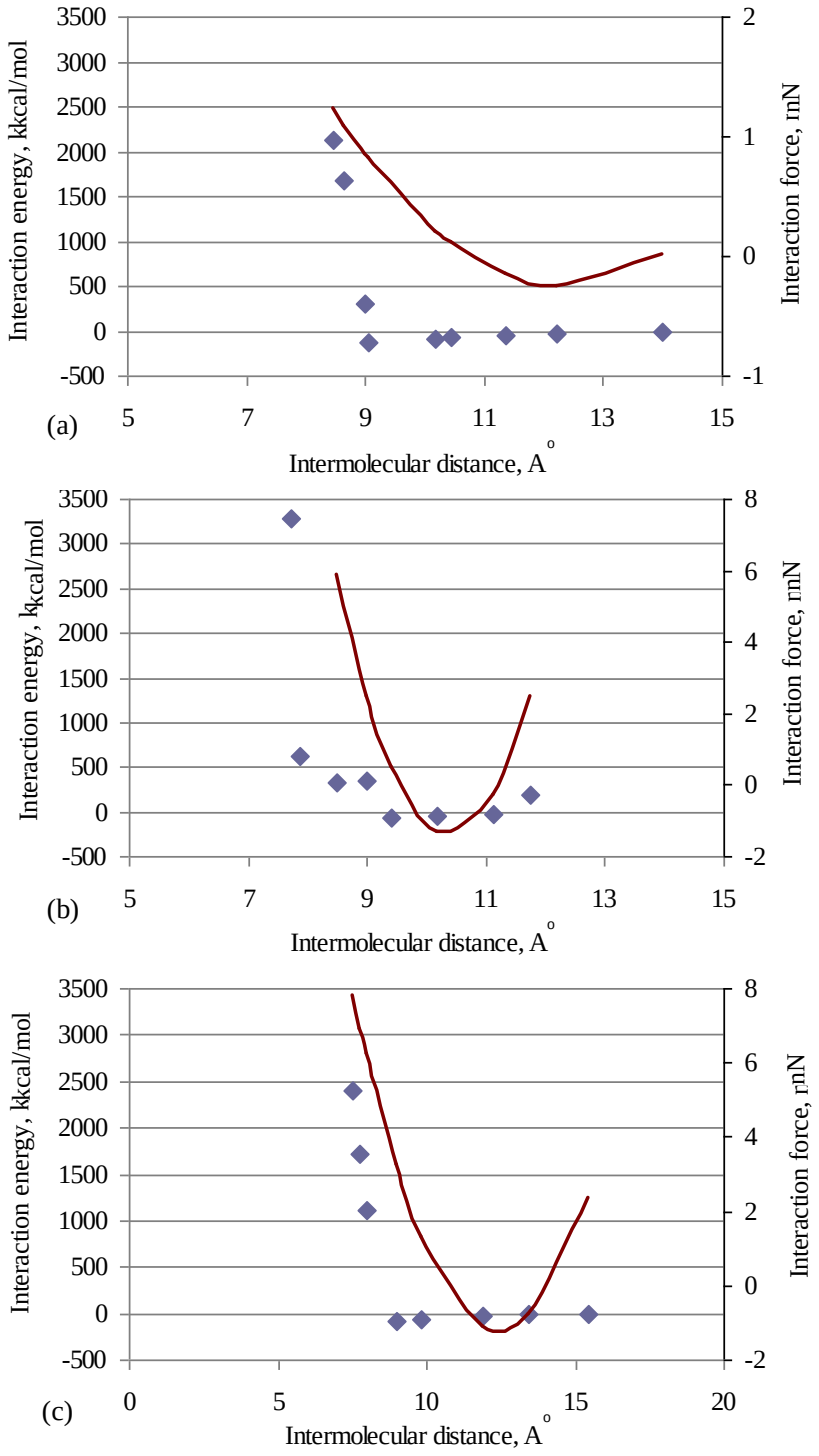

Fig. 3. Interaction energy (diamonds), and interaction force (line) of the BMP - graphene complexes (a - complex with BMP-2, b - coplex with BMP-6, c - complex with BMP-7) as a function of intermolecular distance.

Table 2. Particularities of disulphide bridges involved in the stabilization of BMP monomers

Protein model		Disulphide bonds		
BMP-2	Amino acids involved	Cys^{14}-Cys^{79}	Cys^{43}-Cys^{111}	Cys^{47}-Cys^{113}
	Type*	RHS	LHS	LHS
	Length	2.04 Å	2.06 Å	2.05 Å
BMP-6	Amino acids involved	Cys^{31}-Cys^{97}	Cys^{60}-Cys^{129}	Cys^{64}-Cys^{131}
	Type*	RHS	LHS	LHS
	Length	2.01 Å	2.06 Å	2.05 Å
BMP-7	Amino acids involved	Cys^{38}-Cys^{104}	Cys^{67}-Cys^{136}	Cys^{71}-Cys^{138}
	Type*	RHS	LHS	-
	Length	2.03 Å	2.04 Å	2.03 Å

* RHS: right handed spiral; LHS: left handed spiral

In all the studied cases the interaction energy decreased with the increase of the intermolecular distance until the minimum interaction energy is achieved. Analysing the results presented in Figure 3 one can see that the minimum interaction energy, as well as the corresponding intermolecular distance varied with the type of BMP molecule. The lowest interaction energy of

-119.168 kcal/mol was obtained in case of the BMP-2 - graphene complex. The energy data around the minimum value were further fitted by a third order polynomial function and the interaction force was estimated as the first order derivative with respect to the intermolecular distance. The minimum force values presented in Figure 3 correspond to the maximum attraction forces between the two molecules whitin each complex. According to our results, the highest interaction force (1.31 nN) was obtained for the BMP-6 - graphene complex, followed by the BMP-7 - graphene complex (interaction force of 1.09 nN), while BMP-2 - graphene complex was characterized by the lowest interaction force of about 0.25 nN (Figure 3). In terms of interaction forces between BMP molecules and graphene, our results are close to some experimental results obtained on biomolecules by using the atomic force microscopy technique. In particular, the interaction force between *Escherichia coli* and a specific receptor protein is 0.4-0.9 nN [21], the antigen-antibody binding force ranges from 0.1 to 0.05 nN [22], while the protein complex involved in cell adhesion is characterised by an interaction force of 0.4 nN [23].

4. Conclusions

A detailed *in silico* investigation was carried out to characterize at single molecule level three different osteogenic proteins, BMP-2, BMP-6 and BMP-7. As expected by taking into account the amino acids sequence identity, after performing molecular dynamics simulations to equilibrate the BMP molecules at 37^{o}C, some differences in the secondary and tertiary structures have been found. Anyway, the BMP-2, BMP-6 and BMP-7 seem to generally share the overall folding topology of the transforming growth factor β superfamily. The unbinding simulations indicated a better affinity of BMP-6 for graphene, the unbinding force being by 1.20 and 5.24 higher with respect to BMP-7 and BMP-2, respectively.

The knowledge provided here might be useful for further functional characterizations of BMPs in direct relation with their interaction with other biomolecules such as receptors, regulatory proteins, glycoaminoglycans, etc.

Acknowledgements

This research has been supported by the National Research Grant PN-II-PCCA-140/2012, Ministry of National Education, Executive Agency for Higher Education, Research, Development and Innovation Funding.

References

[1] S. Bose, M. Roy, A. Bandyopadhyay, Trends Biotechnol, **30**, 546 (2012).
[2] Y. Zhang , C. Wu, S. Guo, J. Zhang, Nanotechnology Reviews, **2**, 27 (2013).
[3] D. R. Dreyer, S. Park, C. W. Bielawski, R. S. Ruoff, Chem. Soc. Rev. **39**, 228, (2010).
[4] S. Stankovich, D. A. Dikin, G. H. B. Dommett, K. M. Kohlhaas, E. J. Zimney, E. A. Stach, R. D. Piner, S. T. Nguyen, R. S. Ruoff, Nature, **442**, 282 (2006).
[5] C. Scheufler, W. Sebald, M. Hulsmeyer, J.Mol.Biol. **287**, 103 (1999).
[6] J. M. Wozney, SPINE, **27**, S2 (2002).
[7] J. Greenwald, J. Groppe, P. Gray, E. Wiater, W. Kwiatkowski, W. Vale, S. Choe, Mol.Cell **11**, 605 (2003).
[8] G. P. Allendorph, M. J. Isaacs, Y. Kawakami, J. C. Belmonte, S. Choe, Biochemistry, **46**, 12238 (2007).
[9] E. Lindahl, B. Hess, D. van der Spoel, J. Mol. Mod. **7**, 306 (2001).
[10] R. A. Laskowski, Nucleic Acids Res, **37**, D355 (2009).
[11] R. A.Laskowski, M. B. Swindells, J. Chem. Inf. Model., **51**, 2778 (2011).
[12] W. Humphrey, A. Dalke, K. Schulten, Journal of Molecular Graphics, **14**, 33 (1996).
[13] D. Schneidman-Duhovny, Y. Inbar, R. Nussinov, H.J. Wolfson, Nucleic Acids Res, **33**, W363 (2005).
[14] N. Andrusier, R. Nussinov, H.J. Wolfson, Proteins **69**, 139 (2007).
[15] E. A. Wang, V. Rosen, J. S. D'Alessandro, M. Bauduy, P. Cordes, T. Harada, D. I. Israel, R. M. Hewick, K. M. Kerns, P. LaPan P, et al., Proc Natl Acad Sci U S A, **87**, 2220 (1990).
[16] A. Daluiski, T. Engstrand, M. E.Bahamonde, L. W. Gamer, E. Agius, S. L. Stevenson, K. Cox, V. Rosen, K.M. Lyons, Nat Genet, 27, 84 (2001).
[17] G. N. Ramachandran, V. Sasisekharan, Adv. Protein Chem. **23**, 283 (1968).
[18] W. R. Pearson, D. J. Lipman, PNAS, **85**, 2444 (1988).
[19] J. S. Richardson, Adv. Protein Chem., **34**, 167 (1981).
[20] D. Duhovny, R. Nussinov, H. J. Wolfson, 2'nd Workshop on Algorithms in Bioinformatics(WABI) Rome, Italy, Lecture Notes in Computer Science **2452**, 185, Springer Verlag (2002).
[21] R. Mahmood, M. Elzinga, R. G. Yount, Biochemistry, **28**, 3989 (1989).
[22] A. Vinckier, P. Gervasoni, F. Zaugg, U. Ziegler, P. Lindner, P. Groscurth, A. Pluckthun, G. Semenza, Biophys J., **74**, 3256 (1998).
[23] J. T. Finer, R. M. Simmons J. A. Spudich, Nature, **368**, 113 (1994).